Why Do Losses of Polyatomic Fragments Strongly Dominate Losses of Atoms at High Internal Energies? Methyl versus Cl• Loss from the 2-Chloropropane Cation

C. E. Hudson,[†] J. C. Traeger,[‡] L. L. Griffin,[§] and D. J. McAdoo*,[†]

Marine Biomedical Institute, University of Texas Medical Branch, 301 University Boulevard, Galveston, Texas 77555-1043, Department of Chemistry, La Trobe University, Victoria 3086, Australia, and Department of Marine Sciences, Texas A&M University at Galveston, Galveston, Texas 77553

Received: July 25, 2002

Previous work demonstrates that rates of H• losses generally increase much less rapidly with increasing internal energy than do those of losses of polyatomic fragments. To determine whether this is also the case for the losses of other atoms, the dependencies of the rates of Cl• and CH_3• losses from $CH_3CHClCH_3^{+\bullet}$ on ion internal energy are compared. These dependencies were established experimentally by photoionization mass spectrometry. The reactant ion and the transition states were characterized by B3LYP/6-31G(d), B3LYP/6-311G(d,p), and MP2/6-31G(d) theories. The transition states located are at very long bond lengths and close in energy to the corresponding dissociation products. Rate constants as a function of internal energy were obtained by RRKM theory. According to both experiment and theory, above its onset, methyl loss increases much more rapidly with internal energy than does loss of Cl•. This stems from three vibrational frequencies being substantially lowered in the transition state for the former but not in the latter reaction as they are being transformed into rotations of the separated products. This produces a much more rapid increase in the RRKM sum of states for the transition state to $CH_3CHCl^+ + CH_3$•, and thus also in the rate of that reaction. This, together with previous work, establishes that losses of polyatomic fragments from ions in the gas phase generally increase much faster with increasing internal energy than do losses of atoms.

Introduction

We recently demonstrated by experiment and Rice−Ramsperger−Kassel−Marcus (RRKM) theory that the rates of unimolecular H• losses increase much more slowly with increasing internal energy than do the rates for losses of polyatomic fragments.[1−3] Similarly, Troe noted that, according to his statistical adiabatic channel model, methyl loss from ethane increases much more rapidly with increasing internal energy than does loss of O from NO_2.[4] However, the possibility of a general difference between the rates of unimolecular losses of atoms and larger fragments has not been recognized or addressed. We concluded[1−3] that the relatively slow losses of atoms at high energies stem primarily from fewer vibrational frequencies being lowered in the transition state and those to a lesser extent. These effects can be understood based on the RRKM expression

$$k_E = \frac{N_{(E-E^\circ)}}{h\rho_E} \qquad (1)$$

In this expression, $N_{(E-E^\circ)}$ is the sum of states in the transition state at internal energy E, E° is the activation energy for the reaction, h is Planck's constant and ρ_E is the density of states at E. At higher energies, the relative rates are largely determined by $N_{(E-E^\circ)}$, which in turn is inversely related to the values of the frequencies of the vibrational modes and internal rotations of the transition state. Differences in the lowering of vibrational frequencies in the transition states arise from (1) conversion of only three vibrations to translations in the loss of an atom versus three conversions to translations and three to rotations in the loss of a nonlinear polyatomic fragment and (2) the greater polarizability of the latter produces looser transition states at longer interfragment distances and with lower frequencies of the transitional modes. We previously predicted[2] that all losses of atoms will increase more slowly with increasing internal energy than competing losses of polyatomic fragments with similar thresholds but stated that information on loss of non-H atoms was needed to verify this. Therefore, we here compare the energy dependencies of the rates of losses of Cl• and CH_3• from the 2-chloropropane cation.

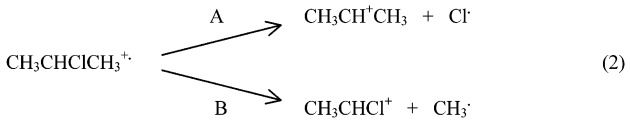

(2)

Methods

Photoionization efficiency (PIE) curves, first differential PIE curves derived from them, and appearance energies (AEs) for the losses of CH_3• and Cl• from the 2-chloropropane cation were obtained as described previously[5,6] at room temperature on a mass spectrometer fitted with a variable wavelength photoionization source.[7] The PI signals were corrected for variation in photon flux as a function of photon energy by multiplying by: [(ion count rate) − (background ion count rate)]/[(photon count rate) − (background photon count rate)]. First differential curves were determined to provide ion abundances as a function of

* To whom correspondence should be addressed. Phone: 409-772-2939. Fax: 409-772-3222. E-mail: djmcadoo@utmb.edu.
[†] University of Texas Medical Branch.
[‡] La Trobe University.
[§] Texas A&M University at Galveston.

10.1021/jp021740s CCC: $25.00
Published on Web 01/01/2003

TABLE 1: Energies Pertinent to the Dissociations of $CH_3CHClCH_3^{+\bullet}$

	MP2/6-31G(d)// MP2/6-31G(d)	B3LYP/6-31G(d)// B3LYP/6-31G(d)	B3LYP/6-311G(d,p)// B3LYP/6-311G(d,p)	ZPE[a]	ΔE[b]	PIE (kJ mol^{-1})[c]
$CH_3CHClCH_3^{+\bullet}$	−577.311615	−578.359507	−578.418599	236	0	0
CH_3CHCl^+	−537.596989	−538.474631	−538.522120	128		
$CH_3^\bullet$	−39.668750	−39.838292	−39.853758	77		
$CH_3CHCl^+ + CH_3^\bullet$	−577.265739	−578.312923	−578.375878	205	81 (91)	125
CH_3CHCl- - -$CH_3^{+\bullet}$	NF[d]	−578.323400	−578.385351	218	69 (77)	
$CH_3CH^+CH_3$	−117.746653	−118.211835	−118.243845	228		
$Cl^\bullet$	−459.552433	−460.136256	−460.166156			
$CH_3CH^+CH_3 + Cl^\bullet$	−577.299086	−578.348091	−578.410001	228	15 (22)	26
$(CH_3)_2CH$- - -$Cl^{+\bullet}$	−577.302501	−578.351354	−578.412172	229	10 (14)	

[a] For B3LYP/6-31G(d) theory, zero-point energies were obtained by multiplying ZPVEs obtained by theory by the scaling factor 0.9806 established by Scott and Radom.[12] For MP2/6-31G(d) theory, zero-point energies were obtained by multiplying zero-point energies obtained by theory by the scaling factor 0.967.[12] [b] Relative energies based on B3LYP/6-311G(d,p)//B3LYP/6-311G(d,p) and B3LYP/6-31G(d)//B3LYP/6- -31G(d) energies; the latter are in parentheses. [c] AE(fragment) − IE($CH_3CHClCH_3$) at 0 K; 0 K values were obtained from the 298 K AEs given in the text by adding 10 kJ mol^{-1} to allow for the thermal energy effective in the dissociation of $CH_3CHClCH_3^{+\bullet}$[14] at 298 K. [d] NF = not found.

molecular ion internal energy.[8,9] Such curves give the rates of the reactions examined at an internal energy equal to the photon energy minus the ionization energy.[8]

Potential energy surfaces for the reactions of interest and relevant vibrational frequencies were explored utilizing the Gaussian 98W suite of programs.[10] B3LYP/6-31G(d) and B3LYP/6-311G(d,p) were used, and MP2/6-31G(d) theory was added for checking because density functional theories sometimes give poor results at extended bond lengths when charge and spin are being separated,[11] as in this work. Higher levels of theory were not applied because the computational demands for locating the transition states with them were prohibitive. The motions of the low-frequency vibrational modes of each stationary point were also analyzed to characterize the transition state modes that are important to increasing the rates of the reactions. The vibrational frequencies obtained were adjusted by multiplication by pertinent scaling factors.[12] RRKM calculations were performed using the program of Zhu and Hase.[13]

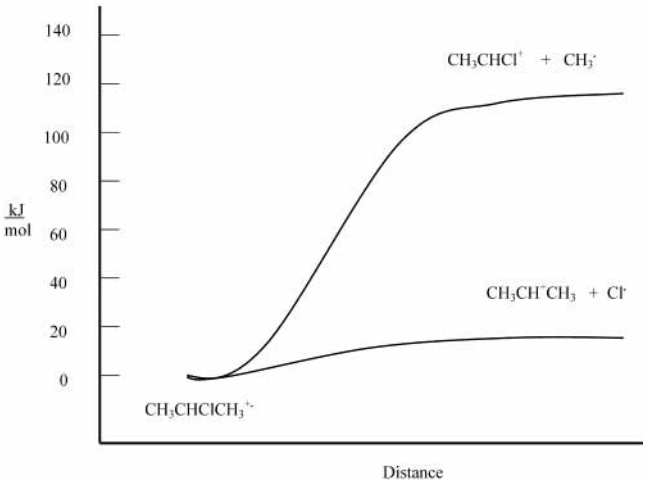

Figure 1. Potential energy diagram for the dissociations of $CH_3CHClCH_3^{+\bullet}$ derived from photoionization ionization and appearance energies.

Results and Discussion

Experimental Energy Dependencies of the Dissociations. The photoionization ionization energy (PIE) obtained for $CH_3CHClCH_3$ is 10.76 ± 0.01 eV; the appearance energy (AE) of (CH_3CHCl^+) is 11.95 ± 0.05 eV, and AE($C_3H_7^+$) is 10.93 ± 0.01 eV. The last value adjusts to a 0 K value of 11.03 eV, agreeing quite well with a recent 0 K AE of 11.085 eV.[14] This dissociation occurs at its thermochemical threshold.[14,15] A potential energy diagram based on the appearance energies is given in Figure 1. A first differential PIE breakdown diagram displaying the relative rates of the dissociations of $CH_3CHClCH_3^{+\bullet}$ of interest is given in Figure 2. At all energies above the onset for its formation, the first differential PIE curves demonstrate that $C_3H_7^+$ formation is dominant. Its rate of formation initially rises rapidly with increasing energy, diminishes quickly, and then rises again above about 11.9 eV. By 13.2 eV photon energy, $C_2H_4Cl^+$ is formed 60% as often as is $C_3H_7^+$, so, despite its ca. 1 eV (ca. 100 kJ mol^{-1}) higher threshold, by about 1.3 eV above the onset for $C_2H_4Cl^+$ formation, that ion and $C_3H_7^+$ are formed at comparable rates, demonstrating that the rate of formation of the former rises faster with internal energy.

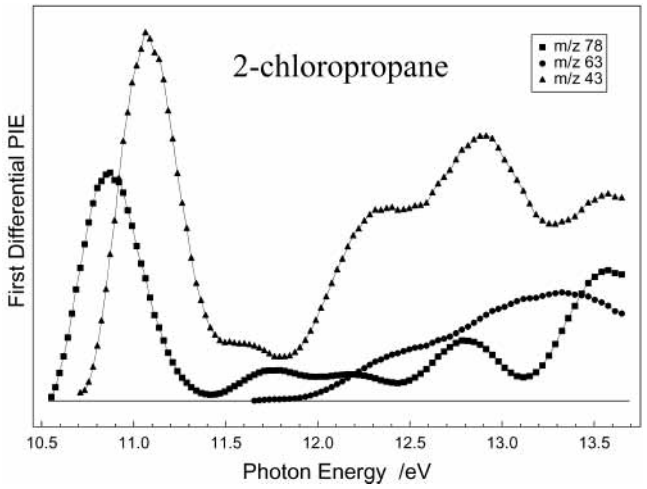

Figure 2. First differential PIE curves for the molecular ion (*m*/*z* 78), $C_2H_4Cl^+$ (*m*/*z* 63), and $C_3H_7^+$ (*m*/*z* 43) giving the energy dependencies of the associated dissociations. These curves were obtained as described in the text. Note that the abundances of *m*/*z* 63 and *m*/*z* 43 are within about a factor of 2 of each other at the higher energies.

Little increase is seen in Figure 2 in the degree of formation of any ion from 11 to 12 eV photon energy, suggesting an absence of electronic states with onsets in that energy range. This supposition is born out by an absence of electronic states of $CH_3CHClCH_3^{+\bullet}$ with onsets between 10.8 and 12.4 eV.[16]

Hybrid Functional and ab Initio Descriptions of the Dissociations of $CH_3CHClCH_3^{+\bullet}$. Geometries (Figure 3) and energies (Table 1) of the reactant, transition states, and products for losses of both $Cl^\bullet$ and $CH_3^\bullet$ were located by three levels of theory. Dissociation energies at the highest level of theory employed, B3LYP/6-311G(d,p), are 12 and 44 kJ mol^{-1} lower than ΔAE values corrected to 0 K. The comparable B3LYP/6-31G(d) differences were 5 and 34 kJ mol^{-1}. MP2/6-31G(d)

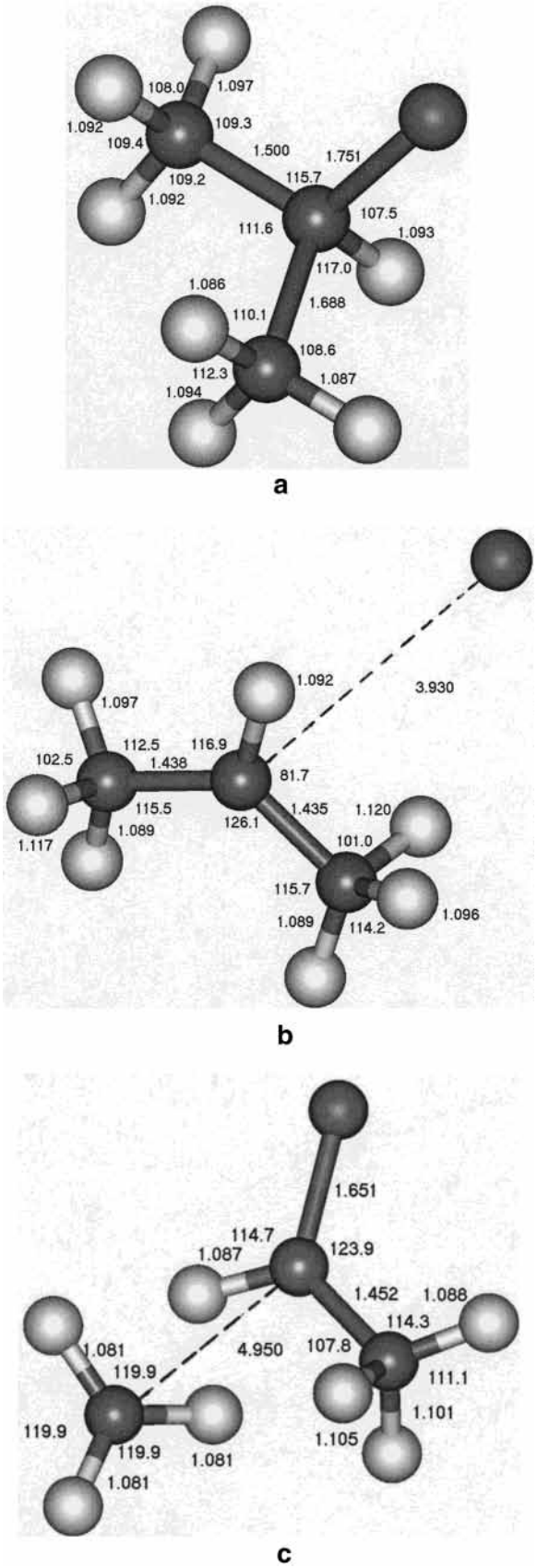

Figure 3. a. B3LYP/6-311G(d,p) geometries of $CH_3CHClCH_3^{+\bullet}$. b. The transition state for Cl loss. c. The transition state for methyl loss. In the third structure, the CH bonds in the departing methyl are all 1.084 Å long and the bond angles are all 119.9°.

dissociation energies differed by 14 and 40 kJ mol^{-1} from those obtained by photoionization and adjusted to 0 K, so B3LYP/6-31G(d) theory gave results closest to experimental ones. The relative energies obtained by the three theories are within 10 kJ mol^{-1} of each other, supporting their mutual accuracy. The larger differences between experiment and theory are for the higher energy process, so competition from the lower energy process (a competitive shift) could have raised $AE(CH_3CHCl^+)$. AEs measured for loss of $Cl^\bullet$ agree to within about 0.05 eV,[14,15] so the good agreement of theory with experiment for that process suggests that reasonable results were obtained by B3LYP/6-311G(d,p) theory, even though there are questions regarding its accuracy for describing dissociating species.[11] Despite considerable effort, a transition state for $CH_3^\bullet$ loss was not located by MP2/6-31G(d) theory. Therefore, that reaction may not have a transition state with an imaginary frequency. If a saddle point transition state does not exist for this reaction, it is likely that an entropic minimum[17,18] with similar frequencies and at a similar energy is rate controlling in this dissociation.

The transition states having one imaginary frequency located here by B3LYP/6-311G(d,p) theory are 12 and 5 kJ mol^{-1} below the energies from the same theory for the corresponding dissociated fragments. IRC calculations at the B3LYP/6-31G(d) level found lower energy regions on either side of TS(−Cl), making this is a real transition state according to theory. However, the IRC did not go all of the way to either the ground state ion or to the fully dissociated fragments (it would not be expected to reach the dissociated products unless there were a reverse barrier to dissociation). The point at which the IRC stopped in the forward direction is 2.3 kJ mol^{-1} below the transition state and that toward the ground state 0.13 kJ mol^{-1} lower. The CCl distance progressed from 3.746 to 3.801 to 4.381 Å as the C−Cl bond extended from the IRC end point nearer the ground state through the transition state to the point at greater distance. Thus, the energy changes are slight over a 0.6 Å change in the length of the breaking bond. The lower energy toward the products suggests the occurrence of a long-range ion−neutral complex in a shallow potential minimum between the transition state and the dissociation products. A pathway from $TS(-CH_3)$ was traced to the ground-state ion by a combination of IRC and ordinary optimization methods. Because the transition states for both dissociations located are at long bond lengths, if there are additional transition states closer to the dissociation products, they should have very similar frequencies and energies to those located.

To obtain frequencies for RRKM calculations and to characterize the lowest frequency vibrations of the transition state, we characterized the vibrational modes of the ground and transition states by B3LYP/6-31G(d), B3LYP/6-311G(d,p), and MP2/6-31G(d) theories. The frequencies obtained for the ground and transition states at the second and third levels of theory are given in ascending order in Table 2, although the frequencies on the same lines in the table do not necessarily arise from corresponding motions in ground and transition states. All levels of theory gave mostly similar vibrational frequencies for $CH_3CHClCH_3^{+\bullet}$ other than those on the 20th line, where a nearly 2-fold discrepancy exists.

Except for the reaction coordinate, similar values of frequencies for the transition state for $Cl^\bullet$ loss were obtained by all of the theories. During the loss of $Cl^\bullet$, marked lowering of the frequency of the vibrational mode that becomes the reaction coordinate and the two others that are becoming translations would be anticipated. However, five frequencies including that of the reaction coordinate are substantially lowered, with the corresponding B3LYP/6-31G(d) frequencies on lines 2−5 in the table having ratios (ground to transition state) of 7.9, 4.1,

TABLE 2: Vibrational Frequencies[a]

	B3LYP/6-311G(d,p)// B3LYP/6-311G(d,p)			MP2/6-31G(d)// MP2/6-31G(d)	
	ground state	TS(−Cl)	TS(−CH_3)	ground state	TS(−Cl)
1	191.5	50.0i	40.6i	223.7	33.1i
2	213.8	27.1	11.4	245.9	40.4
3	237.1	58.3	25.6	271.6	85.4
4	324.1	146.8	39.7	354.7	161.9
5	377.8	186.2	118.1	421.6	259.3
6	460.0	422.4	118.6	679.9	453.8
7	654.1	620.0	123.3	839.3	574.6
8	866.2	706.2	396.4	873.1	652.0
9	912.9	911.9	735.7	885.7	900.2
10	926.1	971.4	779.7	918.5	948.1
11	997.1	1090.6	823.3	1022.7	1058.4
12	1038.2	1208.7	974.7	1084.3	1188.2
13	1130.7	1244.6	1052.4	1235.5	1217.3
14	1305.1	1288.0	1175.0	1304.5	1290.1
15	1317.3	1310.0	1332.6	1373.1	1295.3
16	1387.1	1359.8	1365.3	1380.5	1329.6
17	1394.5	1369.2	1410.7	1420.3	1345.8
18	1427.4	1439.4	1411.0	1435.6	1409.0
19	1458.9	1484.8	1413.2	1441.1	1448.6
20	1471.4	1543.5	1474.8	2611.9	1502.2
21	3005.9	2836.5	2957.1	2932.0	2729.0
22	3028.9	2878.5	3001.2	2958.0	2794.3
23	3055.9	3041.0	3101.3	2976.0	2970.3
24	3087.1	3047.9	3156.4	3024.5	2983.0
25	3126.1	3125.9	3175.6	3051.4	3035.1
26	3163.3	3157.0	3290.1	3117.5	3069.8
27	3212.0	3161.4	3290.4	3122.9	3073.4

[a] The vibrational frequencies obtained by theory were scaled as follows by multiplying by factors established by Scott and Radom.[12] B3LYP/6-311G(d.p) − Frequencies listed are unscaled because appropriate scaling factors do not exist for B3LYP/6-311G(d,p) theory. MP2/6-31G(d) − Frequencies listed were obtained by multiplying those greater than 600 cm^{-1} by 0.9434 and those less than 600 cm^{-1} by 0.9434.[12]

2.2, and 2.0. Thus, two frequencies in addition to those that become translations are substantially reduced during the dissociation and contribute to the increase of the rate constant with internal energy. This contrasts with the situation in transition states for H• losses in which there is little lowering of vibrational frequencies.[1,2] The remaining ground and transition state frequencies are similar to each other.

An analysis of the atomic motions in each of the lower frequency modes in the transition state for Cl• loss reveals that in the reaction coordinate one end of the propyl moves toward Cl and the other end away from it. The 27.1 cm^{-1} mode involves C−Cl bending approximately in the Cl−C2−C1 plane; the 58.3 cm^{-1} mode involves C−Cl stretching; the 146.8 cm^{-1} mode involves twisting around one C−*C* axis to a methyl; and the 186.2 cm^{-1} mode involves a similar motion of the other methyl. Therefore, three frequencies are lowered as a direct result of their association with the extended CCl bond, and the other two are due to less hindered twisting of the incipient isopropyl cation. The latter likely become low-frequency vibrations of the isopropyl cation, whose two lowest frequencies are 122.1 and 136.7 cm^{-1}. Thus, the first three frequencies are markedly lowered by transformation into relative motion of the products, whereas the last two are becoming low-frequency vibrations of $CH_3CH^+CH_3$.

Seven frequencies other than the reaction coordinate are markedly reduced in the transition state for methyl loss. The seven lowest B3LYP/6-31G(d) frequencies excluding those of the reaction coordinate are 1.6 to 19-fold lower in the transition state than are the ground state frequencies on the same lines in Table 2. Because only six vibrations including the reaction coordinate become rotations and translations, two additional vibrational frequencies are substantially lowered in the course of the dissociation, also helping to speed the reaction. The two lowered frequencies in both reactions that are not becoming translations and rotations would influence the energy dependencies of the two reactions similarly, so their effects approximately cancel. Thus, the differential dependence of the rates of the two reactions on internal energy is largely due to the conversion of three vibrations to rotations that occurs only in the loss of the polyatomic fragment.

Examination of the atomic motions as generated by the program in the eight lowest frequency vibrational modes in the transition state including the reaction coordinate for methyl loss permits relating the nature of the transitional modes to bond-breaking, although some of those modes are hard to classify. In the mode with the imaginary frequency, the incipient methyl and CH_3CHCl^+ are moving away and toward each other, consistent with this being the reaction coordinate. The 11.4 cm^{-1} mode is a developing rotation, as the departing methyl is twisting around the CC bond to that methyl with little other motion in the system. The 25.6 cm^{-1} mode is a movement of the departing methyl and Cl end of CH_3CHCl^+ toward each other and the other end of the CH_3CHCl^+ away from that methyl. The 39.7 cm^{-1} mode involves twisting around the C−C bond of CH_3-$CHCl^+$. The 118.1 cm^{-1} mode primarily involves bending such that one of the hydrogens of the departing methyl moves away from the rest of the ion as the other two move toward it and the reverse. The 118.6 cm^{-1} mode is another bending motion such that twisting approximately about a CH bond of the departing methyl moves a second methyl H toward the developing CH_3-$CHCl^+$ and the third one away from it. In the 123.3 cm^{-1} mode, CH_3CHCl^+ is rotating around its C*C* axis. Finally, the mode at 396.4 cm^{-1} is primarily a C−C−Cl bend in CH_3CHCl^+. As would be expected, most of the lowering of vibrational frequencies in the transition state for methyl loss are directly related to the breaking of the CC bond.

RRKM Rates of Dissociation of $CH_3CHClCH_3^+$•. Log rate constant versus internal energy curves for the losses of Cl• and CH_3• derived by RRKM theory are given using critical energies obtained by experiment and frequencies obtained by B3LYP/6-311G(d,p) theory in Figure 4a and using critical energies and frequencies from B3LYP/6-311G(d,p) theory in Figure 4b. In the first calculations, experimental dissociation energies were corrected to 0 K (See Table 1), so they can be compared to the energies provided by theory. The parameters used in these two calculations bracket any other RRKM calculations that could have been performed using parameters obtained in this study.

The rate of Cl• loss is very high near threshold, but it only rises slowly with increasing energy. For that reaction, the ratio in the RRKM rate expression (eq 1) does not rise very rapidly because the sum of states in the transition state and the density of states in the reactant increase similarly with increasing energy. When the experimental critical energies were used, the RRKM rate for methyl loss rose rapidly with increasing energy such that at about 280 kJ mol^{-1} it surpasses the rate of Cl• loss (Figure 4a). A similar log *k* versus *E* curve was obtained (not shown, crossover $E = 220$ kJ mol^{-1}) when the same critical energy was used but the five lowest frequencies were replaced with free rotors. However, using the transition state energies obtained by B3LYP/6-311G(d,p) theory (17 kJ mol^{-1} lower for $C_3H_7^+$ and 56 kJ mol^{-1} lower for CH_3CHCl^+; note that 5 and 12 kJ mol^{-1} respectively of these discrepancies arises from the values employed from theory being below the theoretical dissociation thresholds) shifted the crossover down to about 140 kJ mol^{-1}

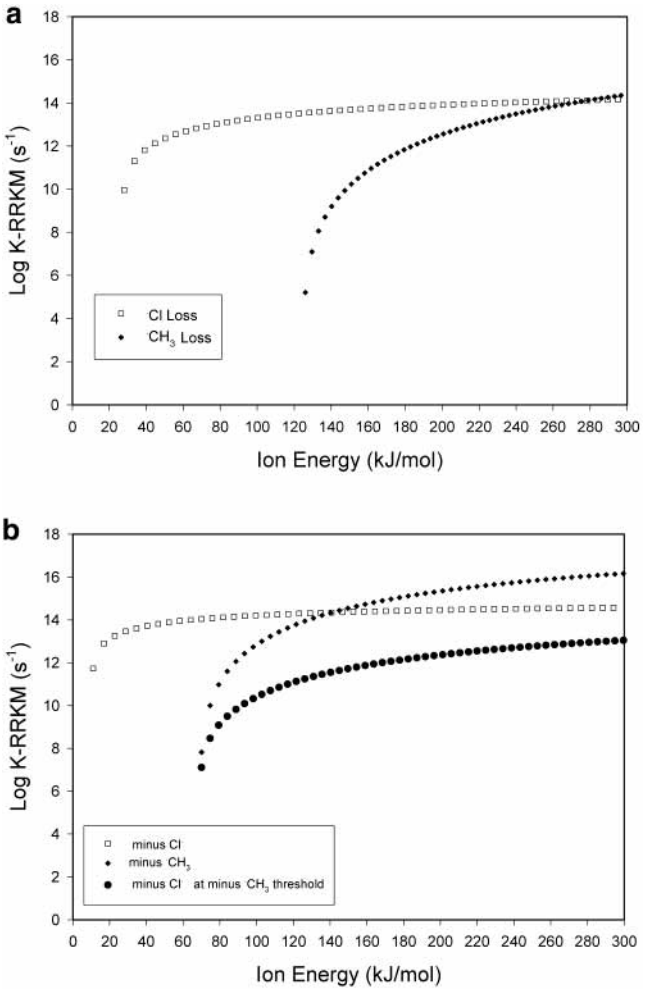

Figure 4. a. log *k* versus internal energy curves obtained by RRKM theory for the losses of Cl• and •CH_3 using experimental critical energies. Note the much slower rate of •CH_3 loss at its threshold and its overtaking of the rate of the other reaction at high energies. b. log *k* versus internal energy curves obtained by RRKM theory for the losses of Cl• (open squares), CH_3• (diamonds), and a hypothetical reaction involving the loss of a fragment with the activation energy of the CH_3• loss and the transition state frequencies of the Cl• loss (filled circles). B3LYP/6-311G(d,p) energies were used for the first two processes. Note the crossover in the curves at about 140 kJ mol^{-1} for the two curves obtained using the actual reaction parameters and the much slower rise of the hypothetical Cl• loss relative to the methyl loss when the two reactions are given the same threshold.

(Figure 4b), so the rate of increase of the latter reaction with increasing energy was even greater using those parameters. Experimentally (Figure 2) the CH_3CHCl^+ abundance is 60% of that of $C_3H_7^+$ at 13.2 eV, an energy content of 245 kJ mol^{-1}. This agrees reasonably with the RRKM crossover energy of 280 kJ mol^{-1} obtained using the experimental critical energy for CH_3CHCl^+ formation and completely unmodified theoretical frequencies. However, this could be fortuitous, as AE(CH_3CHCl^+) may be elevated by a competitive shift (see above). Employing the experimental onset and assuming free rotors also gave good agreement between experiment and RRKM theory. Using transition state energies from theory causes the rate of CH_3CHCl^+ formation to increase more rapidly than observed in Figure 2, so use of critical energies obtained by theory gives results in poorer agreement with experiment. Therefore, it is possible that it is the critical energy from theory that is too low, accounting for the discrepancy between results of RRKM theory and experiment. However, no matter which of the possible parameters are used in RRKM theory, the rate of loss of the polyatomic fragment rises much faster than that of Cl• with increasing internal energy.

Differences in threshold energies and differences in frequencies both influence the rises of RRKM rates with internal energy. Therefore, to isolate the effects of the changes in frequencies, we performed RRKM calculations on a hypothetical reaction with the frequencies of the Cl• loss transition state and the threshold for the methyl loss. The ratio $k(-CH_3\bullet)/k(-Cl\bullet) = 2$ at a common threshold because the denominators in eq 2 would be the same and the numerators would have the ratio 2:1 because there are two ways to lose methyl but only one state leading to Cl• loss at threshold. In this hypothetical situation, the RRKM rate of the reaction with the larger number of transitional modes (methyl loss) increases quite rapidly with increasing energy to become several orders of magnitude faster than Cl• loss at high energies (Figure 4b), further supporting our conclusions.

The polarizability of CH_3• is 2.7 $Å^3$,[18] that of Cl• is 2.18 $Å^3$,[19] and that of H• is 0.67 $Å^3$.[19] The polarizability of Cl• being much greater than that of H• and approaching that of CH_3• affords the opportunity to assess the roles of polarizability of the incipient fragment and the number of transitional modes on the rates of dissociations of ions. The length of the breaking bond in the transition state appears to be inversely related to polarizability of the developing neutral fragment, as the CC distance in the transition state for methyl loss is 4.949 Å (4.786 Å), and the CCl distance in the transition state for losing Cl is 3.864 Å (3.801 Å) (first values B3LYP-6/311G(d,p) theory, Figure 1; values in parentheses are from B3/6-31G(d) theory). In contrast, the C−C distances are 2−3-fold longer than CH distances in the transition states for the dissociations of alcohol ions.[2] Despite their having similar polarizabilities and breaking bond lengths, the loss of methyl increases much faster with increasing internal energy than does the loss of Cl•, further confirming that it is primarily the larger number of transitional modes in the former reaction that gives it its steeper dependence on reactant internal energy.

The results presented here establish that the rates of losses of atoms other than H• also increase in rate much more slowly with increasing energy than do competing losses of polyatomic fragments, and, if all else is equal, the losses of atoms will be much slower than competing processes at high energies. This has been observed in six other systems that we have studied[1−3] and one system studied by another group,[20] and we have yet to find a system that does not display this pattern. Therefore, this phenomenon seems quite general. The difference in the energy dependence of the two types of dissociations occurs primarily because three frequencies are becoming rotations and are thus substantially lowered in transition states for the loss of a polyatomic fragment. The extension of the generalization that atoms are lost more slowly than larger groups at high energies in unimolecular dissociations accomplished here suggests that this might sometimes be a useful guide to selecting reactions for use in the laboratory and in the factory.

References and Notes

(1) McAdoo, D. J.; Olivella, S.; Sole, A. *J. Phys. Chem. A* **1998**, *102*, 10798.

(2) Griffin, L L.; Traeger, J. C.; Hudson, C. E.; McAdoo, D. J. *Int. J. Mass Spectrom.* **2002**, *217*, 23.

(3) Hudson, C. E.; McAdoo, D. J.; Griffin, L. L.; Traeger, J. C. *J. Am. Soc. Mass Spectrom.* In press.

(4) Troe, J. *J. Chem. Phys.* **1983**, *79*, 6017.

(5) Traeger, J. C.; McLoughlin, R. G. *J. Am. Chem. Soc.* **1981**, *103*, 3647.

(6) Traeger, J. C.; Morton, T. H. *J. Am. Chem. Soc.* **1996**, *118*, 9661.

(7) Traeger, J. C. *Int. J. Mass Spectrom. Ion Processes* **1984**, *58*, 259.

(8) Hurzeler, H.; Inghram, M. G.; Morrison, J. D. *J. Chem. Phys.* **1958**, *28*, 76.
(9) Traeger, J. C.; Hudson, C. E.; McAdoo, D. J. *J. Am. Soc. Mass Spectrom.* **1995**, *7*, 73.
(10) Frisch, M. J.; Trucks, G. W.; Schlegel, H. B.; Scuseria, G. E.; Robb, M. A.; Cheeseman, J. R.; Zakrzewski, V. G.; Montgomery, J. A., Jr.; Stratmann, R. E.; Burant, J. C.; Dapprich, S.; Millam, J. M.; Daniels, A. D.; Kudin, K. N.; Strain, M. C.; Farkas, O.; Tomasi, J.; Barone, V.; Cossi, M.; Cammi, R.; Mennucci, B.; Pomelli, C.; Adamo, C.; Clifford, S.; Ochterski, J.; Petersson, G. A.; Ayala, P. Y.; Cui, Q.; Morokuma, K.; Malick, D. K.; Rabuck, A. D.; Raghavachari, K.; Foresman, J. B.; Cioslowski, J.; Ortiz, J. V.; Stefanov, B. B.; Liu, G.; Liashenko, A.; Piskorz, P.; Komaromi, I.; Gomperts, R.; Martin, R. L.; Fox, D. J.; Keith, T.; Al-Laham, M. A.; Peng, C. Y.; Nanayakkara, A.; Gonzalez, C.; Challacombe, M.; Gill, P. M. W.; Johnson, B. G.; Chen, W.; Wong, M. W.; Andres, J. L.; Head-Gordon, M.; Replogle, E. S.; Pople, J. A. *Gaussian 98*; Gaussian, Inc.: Pittsburgh, PA, 1998.
(11) Bally, T.; Sastry, G. N. *J. Phys. Chem. A* **1997**, *101*, 7923.
(12) Scott, A. P.; Radom, L. *J. Phys. Chem.* **1996**, *100*, 16502.
(13) Zhu, T. L.; Hase, W. L. *Quantum Chemistry Program Exchange*; Chemistry Department, University of Indiana: Bloomington, IN, 1993; p 644.
(14) Baer, T.; Song, Y.; Ng, C. Y.; Liu, J.; Chen, W. *J. Phys. Chem. A* **2000**, *104*, 1959.
(15) Traeger, J. C. *Int. J. Mass Spectrom. Ion Phys.* **1980**, *32*, 309.
(16) Kimura, K.; Katsumata, S.; Achiba, T.; Iwata, S. *Handbook of Helium (He I) Photoelectron Spectra of Fundamental Organic Molecule. Ionization Energies, ab initio Assignments, and Valence Electronic Structure for 200 Molecules*; Japanese Scientific Societies Press: Tokyo, Japan, 1981.
(17) Bowers, M. T.; Jarrold, M. F. J.; Wagner-Redeker, W.; Kemper, P. R.; Bass, L. M. *Faraday Discuss. Chem. Soc.* **1983**, *75*, 57.
(18) Klots, C. E. *J. Chem. Phys.* **1976**, *64*, 4269.
(19) Nagle, J. K. *J. Am. Chem. Soc.* **1990**, *112*, 4740.
(20) Booze, J. A.; Schweinsberg, M.; Baer, T. *J. Chem. Phys.* **1993**, *99*, 4441.